Processing of advanced Al/SiC particulate Metal Matrix Composites under intensive shearing – a novel Rheo process

S. Tzamtzis[1*], N. S. Barekar[1, 2], N. Hari Babu[1], J. Patel[1], B. K. Dhindaw[2], Z. Fan[1]

[1] *BCAST (Brunel Centre for Advanced Solidification Technology), Brunel University, Uxbridge, Middlesex UB8 3PH, UK*

[2] Department of Metallurgical and Materials Engineering, Indian Institute of Technology, Kharagpur, 721302, India

---

Abstract

Particulate Metal Matrix Composites (PMMCs) have attracted interest for application in numerous fields. The current processing methods often produce agglomerated particles in the ductile matrix and as a result these composites exhibit extremely low ductility. The key idea to solve the current problem is to adopt a novel Rheo-process allowing the application of sufficient shear stress (τ) on particulate clusters embedded in liquid metal to overcome the average cohesive force or the tensile strength of the cluster. In this study, cast A356/SiC_p composites were produced using a conventional stir casting technique and a novel Rheo-process. The microstructure and properties were evaluated. The adopted Rheo-process significantly improved the distribution of the reinforcement in the matrix. A good combination of improved Ultimate Tensile Strength (UTS) and tensile elongation (ε) is obtained.

Keywords: A. Metal matrix composites; B. Mechanical properties; Intensive shearing; Particle distribution

---

*Corresponding author. Tel.: +44 1895 266231; fax: +44 1895 269758.

E-mail address: spyridon.tzamtzis@brunel.ac.uk (S. Tzamtzis)

1. Introduction

The mechanical properties that can be obtained with Metal Matrix Composites (MMCs) in combination with their relatively low cost have made them attractive for numerous applications in various fields including aerospace, automotive and sports industries [1,2]. More specifically, particulate MMCs (PMMCs) have been shown to offer improvements in strength, wear resistance, structural efficiency, reliability and control of physical properties such as density and coefficient of thermal expansion, thereby providing improved engineering performance in comparison to the un-reinforced matrix [1-7]. PMMCs are attractive not only for their aforementioned mechanical properties, but also because of the low cost availability of reinforcements. Furthermore, problems associated with the continuously reinforced MMCs, such as fibre damage, microstructural non-uniformity, fibre-to-fibre contact and extensive interfacial reactions can be avoided [5]. PMMCs offer isotropic properties with an increase in strength and stiffness compared to unreinforced materials. However, the less than optimum ductility of MMCs and their fracture behaviour are issues that have to be dealt with.

One of the major challenges when processing MMCs is achieving a homogeneous distribution of reinforcement in the matrix as it has a strong impact on the properties and the quality of the material [8]. To obtain a specific mechanical/physical property, ideally, the MMC should consist of fine particles distributed uniformly in a ductile matrix and with clean interfaces between particle and matrix. However, the current processing methods often produce agglomerated particles in the ductile matrix and as a result they exhibit extremely low ductility [9,10]. Clustering leads to a non-homogeneous response and lower macroscopic mechanical properties. Particle clusters act as crack or decohesion nucleation sites at stresses lower than the matrix yield strength, causing the MMC to fail at unpredictable low stress levels [11,12]. Possible reasons resulting in particle clustering are chemical binding, surface energy reduction or particle segregation [13].

MMCs are generally processed with liquid metal routes such as stir casting and infiltration. A powder metallurgy route is also used for specific applications. However, an infiltration route is the most commonly used method by industry and accounts for the largest volume in primary production [7]. One of the problems associated with the infiltration route is the high volume fraction of the reinforcement which requires additional processes to dilute the content to the required levels. Prolonged processing times and increased processing steps at elevated temperatures aid the chemical reactions between matrix and particle, which often result in brittle secondary phases [14].

Generally, to fabricate high quality MMCs with desirable mechanical properties important factors such as the poor wettability and chemical reactions between the matrix and the reinforcement and the introduction of porosity during the incorporation of the particles require considerable attention [8,15]. Several researchers have tried to optimize the process parameters in order to obtain a uniform distribution of the reinforcement [16-18], whilst others investigated the wettability of reinforcement particles by the matrix alloy [19] and the distribution of the reinforcement as affected by the interaction between the solidification conditions and the particles [20,21]. The particle size also plays a significant role in the final distribution of the particles. The agglomerative nature of ultrafine particles due to their high cohesive energy leads to an increase in the total surface area and increases their tendency to clump together forming agglomerates and clusters [22,23], inducing an unwanted brittle nature to MMCs.

The target of this study is to overcome problems that exist currently in the processing of PMMCs and produce advanced Al/SiC composites with high quality microstructures, a uniform distribution of the reinforcement throughout the whole sample and good mechanical properties of the final product. The key idea is to apply sufficient shear stress (τ) on particle clusters embedded in the liquid metal to overcome the average cohesive force or the tensile strength of the cluster. Molecular dynamics studies [24-26] suggest that the intensive shearing can displace the position of atoms that are held together with high strength bonds. Under a high shear and high intensity of turbulence, liquid can penetrate into the clusters and displace the individual particles within the cluster. A new Rheo-process is introduced for the production of Al/SiC PMMCs utilizing the MCAST (melt conditioning by advanced shear technology) process, developed at Brunel Centre for Advanced Solidification Technology (BCAST), Brunel University, in which the liquid undergoes a high shear stress and high intensity of turbulence inside a specially designed twin-screw machine [27,28].

2. Experimental details

2.1 Materials

Commercially available casting Al-alloy A356 was slightly modified (actual composition: Al-7.50Si-0.30Mg-0.003Cu-0.05Fe-0.005Mn-0.003Zn-0.11Ti, in wt.%) and used as the matrix material for the current study. Additions of an Al-46.45 wt.% Fe master alloy did not affect the alloy composition other than the Fe levels and were used to facilitate ejection and help die release in high-pressure diecasting (HPDC) [29]. The specific alloy was chosen because a Si content of at least 7 wt.% in the Al matrix is required to prevent or delay the formation of aluminium carbide during processing of Al/SiC composites for temperatures up to 750°C [30]. The reinforcement used was black SiC_p (average particle size 4μm), supplied by Electro Abrasives.

2.2 Equipment

A top loaded resistance furnace was used for melting, mixing and reheating the materials in flat bottom, cylindrical graphite crucibles. The first part of the fabrication process was conventional mechanical stirring for the distributive mixing of the reinforcement in the matrix. The mixing equipment for this stage consisted of a driving motor capable of producing a rotation speed within the range of 0-1300rpm, a control part for for the vertical movement of the impeller and a transfer tube used for introducing the ceramic powders in the melt. Since the impeller design plays a crucial role [31], an axial flow impeller was used with the impeller diameter being equal to 0.4 times the diameter of the vessel based on a previous study for flat bottom vessels [32].

For the second and novel part of the processing, a twin-screw machine was used for the dispersive mixing of the SiC particles in the liquid. The twin-screw machine has a pair of co-rotating, fully intermeshing and self-wiping screws rotating inside a barrel. The screws have specially designed profiles to achieve a high shear rate and high intensity of turbulence [27,28]. Figure 1 shows a schematic illustration of the equipment used for both processes.

2.3 Processing

2.3.1 Compocasting - Distributive Mixing

A356 alloy ingots were melted in graphite crucibles, using a top loaded resistance furnace at a temperature of 700°C. The melt was kept at the preset temperature for approximately 2h for homogenisation of temperature and composition. A controlled argon atmosphere was maintained inside the furnace throughout the whole experiment to prevent melt oxidation. At the same time the SiC powder was preheated in a furnace set at 400°C for approximately 30 minutes to remove surface impurities and assist in the adsorption of gases. The ceramic particles were then poured slowly and continuously into the molten metal *via* a vortex introduced by mechanical agitation and the melt was continuously stirred at 600-800rpm. To improve wettability, mixing was carried out in both the liquid and semisolid states. The impeller was frequently moved vertically within the mixture to ensure a uniform distribution of the particles. The conventional mechanical stirring of MMCs is very important for the incorporation and distributive mixing of the ceramic particles in the metal matrix.

After all the SiC powder was introduced successfully in the liquid metal, the composite mixture was allowed to solidify in the crucible and subsequently reheated to the preset melting temperature and held there for approximately 30 minutes. It was then stirred for 2 minutes at approximately 300rpm and cast. Two casting methods were used for the composites produced with the distributive mixing process:

1) Composites were cast in a pre-heated cylindrical steel mould and will be referred to as 'compocast' composites.

2) The liquid was transferred into a 280-tonne cold chamber high pressure die casting (HPDC) machine (LK Machinery, Hong Kong), to produce standard tensile test samples. For all the experiments in this study, the die temperature was kept at 220°C. The samples cast with this method will be referred to as 'HPDC' composites.

2.3.2 Rheo process – Dispersive mixing

The Rheo-process for the fabrication of advanced MMCs innovatively adapts a high shear dispersive mixing action of the twin-screw mechanism used for the MCAST process, to the task of the *in situ* creation of a uniformly mixed composite melt followed by direct shaping of the mixture into a near-net shape component using the existing cold chamber HPDC process.

The twin-screw machine was operated at a temperature of 630°C. The rotation speed of the twin-screws was 800 rpm and the shearing time varied between 60 and 180s. The composite mixture was sheared in the twin-screw machine for the predetermined period of time followed by:

1) Casting in a pre-heated cylindrical steel mould. These composites will be referred to as 'MC-cast' in this study, where MC stands for Melt Conditioned.

2) Casting in the HPDC machine to produce standard tensile test samples. These composites will be referred to as 'MC-HPDC'.

The target of the Rheo-process for MMC fabrication is to utilize the high shearing effect of the MCAST process for the dispersion of the ceramic particles within the metal matrix which would lead to a homogeneous distribution throughout the microstructure. The high shear rate and high intensity of turbulence present inside the twin-screw machine barrel are expected to break down any clusters formed during the addition of the reinforcement particles in the metal matrix.

2.4 Metallographic Characterization

Specimens for microstructural characterization were cut from different positions of the final casting. The microstructure was examined by optical microscopy (OM), using a Carl Zeiss Axioskop 2 MAT microscope, and scanning electron microscopy (SEM), using a Zeiss Supra 35VP FEG microscope. The specimens for OM and SEM were prepared by the standard technique of grinding with SiC abrasive paper and polishing with an Al_2O_3 suspension solution and diamond solutions of different particle size (6μm, 3μm, 1μm and 0.25μm).

For the quantitative analysis of the distribution of the reinforcement particles in the metal matrix of the composite, two different statistical methods were used, the first method uses the well known Lacey index [33], whilst the second is a statistical method for analysing spatial dispersions called the Quadrat method [34].

The two extremes of a mixture can be described as completely segregated when any sample withdrawn from the mixture will be composed of a pure component, or fully randomized when the probability of finding a constituent in every point is identical. According to Lacey [35], for a completely segregated mixture the variance S_0^2 can be expressed as:

$$S_0^2 = pq \,, \tag{1}$$

where p and q are the proportions of the two components estimated from the samples. For a fully randomized mixture the variance S_R^2 is:

$$S_R^2 = \frac{pq}{N} \,, \tag{2}$$

where N is the number of particles in the sample. The Lacey index is defined as:

$$M = \frac{S_0^2 - S^2}{S_0^2 - S_R^2} \left(= \frac{\text{How much mixing has occured}}{\text{How much mixing could occur}}\right) , \tag{3}$$

where S^2 is the variance of the mixture. The index should have a zero value for a completely segregated mixture and increase to unity for a fully randomized mixture. A criticism of the Lacey index is that it is insensitive to mixture quality. Practical values of the Lacey index are restricted to the range of 0.75 to 1.0 [36].

For the Quadrat method, the image area to be studied was divided into a number of square cells (quadrats), determined by the simple rule that the quadrat size should be approximately twice the size of the mean area per particle [37]. The number of particles per quadrat, N_q, was measured and then we calculated the skewness β of the N_q distribution, defined by:

$$\beta = \frac{q}{(q-1)(q-2)} \sum \left(\frac{N_{qi} - N_q^{mean}}{\sigma} \right)^3 , \tag{4}$$

where q is the total number of quadrats studied, N_{qi} is the number of particles in the *ith* quadrat (i=1,2,…,q) N_q^{mean} is the mean number of particles per quadrat and σ is the standard deviation of the N_q distribution. According to a previous study [38], an increase in the skewness is indicative of an increase in particle clustering.

The quadrat method was performed on 40 images of different areas of each sample at 500X magnification. A 36-quadrat grid was placed on the examined image covering an area of 924 x 924 pixels in size, the quadrat side being 20μm (154 pixels). To minimize edge effects, particles only inside and in contact with the left and bottom side of each quadrat were counted. A characteristic example of how the Quadrat method was applied on the micrographs can be seen in Figure 2.

3. Results and discussion

3.1 Microstructure

3.1.1 Distributive mixing

Several experiments to optimise the distributive mixing process have shown that it is essential mixing is carried out in the semisolid state to improve the wettability of the SiC particles by the molten Al-alloy. The rotation of the stirrer generates a vortex through which the SiC particles are drawn into the melt. A high and local shear is exerted on the clusters helping break down aggregates of bulk cohesive SiC powder. The maximum force on a particle cluster rotating in a shear flow, in the vicinity of the stirrer is given by [36]:

$$F = 6\pi\eta\alpha^2 \dot{\gamma} , \tag{5}$$

where α is the radius of each primary particle in the cluster, η is the viscosity and $\dot{\gamma}$ is the shear rate in the surrounding liquid medium. The degree of mixing is affected by the distance of the clusters from the stirrer. Whilst a high shear force can be applied to the liquid that is in contact with the impeller, velocity gradients within the liquid media result in low shear force when averaged out of the whole volume of the liquid. Thus mixing is limited for the clusters located away from the impeller, resulting in the characteristic microstructures seen in Figure 3.

In microstructures of the distributive mixed composites, the reinforcement particles have agglomerated forming clusters preferentially located at the grain boundaries or the interdendritic regions regardless of the casting method. This can be attributed to the pushing of the particles by the solidification front and is in accordance with various previous studies [13,21,39-41]. The difference between the two casting methods is that in the case of HPDC, owing to the higher cooling rates leading to a more refined microstructure, the macroscopical segregation observed is significantly lower than in the compo-cast composites. Thus, at lower magnifications, the HPDC samples seem to have a more uniform distribution of the reinforcement. However, with an increase in the magnification, the presence of particle clusters is clearly visible.

Another observation is the high level of porosity in the compo-cast samples. During the conventional mixing process, air bubbles are sucked into the melt via the vortex created while adding the ceramic powder to the melt resulting in porosity in the composite. The particles tend to become attached to the air-bubbles leading to the formation of particle-porosity clusters, especially in low volume fraction composites [42]. Also, there is normal casting porosity resulting from dissolved gases or shrinkage. In the HPDC samples, due to the application of high pressure the levels of porosity are reduced.

3.1.2 Rheo process - Dispersive mixing

As described previously in the distributive mixing process, the shear force applied on the composite mixture by the impeller is not enough to break down all of the SiC clusters. Intensive shearing is required to break down the agglomerates into individual particles by applying a shear stress (τ) that will overcome the average cohesive force or the tensile strength of the cluster. According to Kendall's model [43], the strength of a cluster is:

$$\mathrm{T} = \frac{11.03\varphi^{2}\Gamma_{c}^{5/6}\Gamma^{1/6}}{(l_{f}a)^{1/2}}, \tag{6}$$

where φ, a, Γ_c , Γ, and l_f are the volume fraction of particulates, agglomerate size, fracture surface energy, equilibrium surface energy and the flaw/void size in a cluster respectively. Previous work has measured the tensile strength of highly cohesive particles to be a maximum of 300 kPa [44]. Rumpf [22] calculated the tensile strength of a cluster suggesting that $\mathrm{T} \propto F_c / d^2$, where F_c is the interparticle cohesive force and d is the diameter of the individual particle. According to this, for a smaller particle size and shorter interparticle distance, which is the case for a fine powder, the tensile strength is much higher making the application of a high shear stress important in order to break the clusters.

This can be achieved by the proposed Rheo-process, which uses a specially designed twin-screw machine. The description of the dynamics of fluid flow in twin-screw extruders is quite complex [45]. In the closely intermeshing, self-wiping and co-rotating twin-screw machine used in this study, the fluid flow characteristics are unusual. It has been shown [28] that the fluid moves in the periphery of the screws in what has been described as '*figure 8*' motions moving from one pitch to the next. This way a '*figure 8*' shaped-helix is formed and pushes the fluid along the axial direction of the screws to what is referred to as a positive displacement pumping action. In the continuous flow field, the fluid undergoes cyclic stretching, folding and reorienting processes. Also, in the axial section the fluid follows a circular flow pattern. All these fluid flow characteristics described are schematically illustrated in Figure 4.

The shear rate between the screw and the barrel in a twin screw slurry maker can be estimated by the following equation:

$$\tau = \eta\pi \mathrm{N}(\frac{D}{G} - 2) \, , \tag{7}$$

where η is the viscosity, N is the rotation speed of the screw, D is the outer diameter of the screw, and G is the gap between the screw flight and the barrel surface. From equation (7) it is clear that an increase in the viscosity of the processed liquid and/or an increase in the rotation speed of the screws will increase the shear rate, which has been found to range from approximately 300kPa to 44MPa for Al-alloys. The combination of the fluid dynamics briefly described above and the increased contact surface compared to conventional stirrers contribute to the high shear dispersive mixing action of the twin-screw, capable of breaking down the clusters formed by the SiC particles and resulting in more homogeneous composite microstructures.

Typical microstructures can be seen in Figure 5. The microstructures obtained after the dispersive mixing show a more uniform distribution compared with the distributive mixing process. The MC-cast samples have high levels of porosity similar to the compo-cast ones. This is due to the fact that the distributive mixing process, prior to the Rheo-processing of the composites, causes the suction of air bubbles as mentioned before. The casting method also induces porosity in the samples.

However, for the MC-HPDC samples the resulting microstructures were highly improved. The uniform dispersion of the SiC particles in the matrix is clearly seen in Figure 5(b). It is important to mention that the MC-HPDC composites have a uniform microstructure not only throughout the cross-sections examined but throughout the whole area of the final component, as shown in Figure 6.

It is noticeable in Figure 7 that the majority of the SiC particles are present at the grain boundaries and the interdendritic regions, as expected. However, apart from these there is a large number of SiC particles of a finer size present in the aluminium grains. These particles are approximately 2μm in size, which is within the particle size distribution as given by the supplier. This occurred because the velocity of the solidification front was higher than the critical velocity required for the engulfment of the SiC particles.

After the microstructural analysis of the MC-HPDC samples under the optical microscope, further SEM analysis has revealed interesting features of the microstructure. Two significant observations can be made whilst examining the SEM microstructures:

1) Not all of the dark in contrast particles seen under the optical microscope and assumed to be SiC particles are actually SiC particles. Some of them are α-AlFeMnSi compound particles (Figure 8a). This explains the higher concentration of the particles seen in Figure 3 and Figure 5.

2) The eutectic Si has a very fine spheroidised morphology, with an average size less than 1μm (Figure 8b).

For the vast majority of Al alloys the presence of Fe is detrimental to the mechanical properties and especially ductility. This is attributed to the low solubility of Fe in the α-Al solid solution phase (0.04 wt.%) and its strong tendency to form various Fe-containing compounds [46]. More specifically, ternary Al-Fe-Si phases, such as the hexagonal α-AlFeSi (Al_8Fe_2Si) and the monoclinic β-AlFeSi (Al_5FeSi), are very important in Al-Si based alloys. The presence of Mn is known to stabilise a cubic ternary α-AlMnSi ($Al_{15}Mn_3Si_2$) compound which consumes Fe by forming an equilibrium quaternary phase , α-AlFeMnSi ($Al_{15}(Fe,Mn)_3Si_2$) [47]. Previous work [29] has shown that the MCAST process modifies the morphology of this primary intermetallic compound from dendritic to equiaxed, improving the ductility of the alloys.

Several authors [6,20,40,41] have reported on the heterogeneous nucleation of eutectic Si on SiC particles. The lower thermal conductivity and heat diffusivity of SiC compared to liquid aluminium leads to retention of heat in the SiC particles. As a result their temperature is higher than that of the surrounding liquid, delaying its solidification. Nucleation of the α-Al phase will start in the liquid at a distance away from the SiC particles where the temperature is lower. The growth of the α-Al nuclei leads to enrichment of Si in the areas where SiC is located. As Si can nucleate at a higher temperature compared to aluminium, SiC particles can act as heterogeneous nucleation sites for Si. When the growing Al dendrites push the SiC particles in the eutectic liquid, the relative amount of SiC there is higher causing a severe refinement of the eutectic Si. In this current study, the Si particles were considered to have an elliptical shape, with an average size of its major axis a = 0.7μm and an aspect ratio of minor to major axis b/a = 0.66. To our knowledge, formation of such fine Si particles has not been observed before.

3.2 Quantitative Metallography

The quantitative analysis of the composite microstructures was not focused solely on the SiC particles added in the Al-matrix. Since the Rheo-process changes the morphology of the intermetallic compounds, we believe that a uniform dispersion of all the particles present in the matrix will improve its mechanical behaviour. Consequently, when we refer to particle distribution in this section, we refer to the SiC particle and α-AlFeMnSi intermetallic compound distribution.

The results of the Lacey index M for the distributive and the dispersive mixing are presented in Figure 9 as a function of shearing time. As mentioned previously, the Lacey index is insensitive to mixture quality. The Lacey index of the compo-cast composites (corresponding shearing time of 0s) is 0.906 which is lower than that of the MC-cast, which ranges between 0.955-0.961. This is in agreement with the microstructural observations. For the HPDC and the MC-HPDC composites on the other hand, the results of the Lacey index are not representing the microstructural observations. The distribution of the particles is definitely improved compared to the composites cast in the steel moulds as seen by the overall increase in the Lacey index. However, the improvement in the distribution of the Rheo-processed ones is not reflected. To overcome this problem, further quantitative analysis was carried out on the HPDC and the MC-HPDC composites using the Quadrat method.

The results of the Quadrat method and the skewness calculations are in accordance with the optical observations made from the microstructure. They are given in Figure 10 as a frequency scatter of the number of particulates per quadrat, N_q, together with the corresponding theoretical curves. The magnitude of clustering affects the shape of the N_q distribution, with a higher clustering tendency making the N_q distribution less symmetric. As proven mathematically [34], a clustered spatial distribution follows the negative binomial model, a random spatial distribution follows the Poisson model and a regular spatial distribution model follows the binomial model. The observed particle distribution for the HPDC samples lies closer to the negative binomial curve indicating clustering, whereas the the MC-HPDC sample particle distribution is more of a resemblance to the Poisson the Poisson and binomial curves. It can be seen from these results that the Rheo-process offers a great advantage for the fabrication of the composites producing samples with a better distribution of the particulates compared to conventional methods resulting in more homogeneous microstructures.

Figure 11 shows the variation in β with shearing time. The skewness β calculated for the HPDC samples is significantly higher than that for the MC-HPDC ones, representing the clustering tendency observed. At a shearing time of 0s corresponding to the HPDC produced samples we get a skewness value of 0.821 which then drops to 0.353 for 60s of intensive shearing. For 120s of shearing the value of β is 0.234, while the lowest skewness value of 0.199 is obtained after intensive shearing of the composite melt for 180s.

3.3 Mechanical Properties

An improvement in the distribution of the particles within the Al-matrix will have a positive effect on the mechanical properties of the composites. Vickers hardness measurements on the distributive and dispersive mixed composites confirmed this. As seen from the results in Table 1, the improved distribution of the particles accounts for an increase in the hardness values in both the steel mould cast and the die-cast composites.

The samples produced with the Rheo-process have a much more homogeneous microstructure, the particles being distributed more uniformly throughout the whole volume of the sample. This was consequently reflected in the mechanical properties acquired by the tensile tests carried out. Figure 12 shows a comparison of the mechanical properties of A356/SiC composite samples produced by the two different processes. The MC-HPDC composites show an increase in the tensile elongation together with an increase in the ultimate tensile strength (UTS) of the material, resulting from the effective dispersion of the particles. The magnitude of this increase is about 15%.

4. Conclusions

Advanced Al/SiC_p composites were fabricated following two different routes: (i) a distributive mixing process (compocasting) and (ii) an adopted Rheo-process based on the innovative technology developed by BCAST. The distribution of the SiC particles in the metal matrix was improved significantly when the composites were produced via the Rheo-process. Quantitative image analysis revealed the improved particle distribution of the Rheo-processed composites

It is suggested that the improvement of the reinforcement distribution is a result of the high shearing effect of the specially-designed twin-screw machine in BCAST. The high shear rate and the high intensity of turbulence created by the twin screws in the barrel lead to the uniform dispersion of the reinforcement by breaking up the clusters which are formed whilst adding the SiC particles in the molten metal. This was reflected in the improved combination of mechanical properties of the composites.

Acknowledgements

Financial support from EPSRC is gratefully acknowledged.

References

[1] Clyne TW, Withers PJ. An introduction to Metal Matrix Composites. Cambridge: Cambridge University Press, 1993.

[2] Miracle DB. Metal matrix composites – From science to technological significance. Compos Sci Technol 2005;65:2526-2540.

[3] Lloyd DJ. Particle reinforced aluminium and magnesium matrix composites. Int Mater Rev 1994;39:1-23.

[4] Rohatgi P. Cast metal matrix composites: Past, present and future. AFS Trans 2001:01-133.

[5] Ibrahim IA, Mohamed FA, Lavernia EJ. Particulate reinforced metal matrix composites – a review. J Mater Sci 1991;26;1137-1156.

[6] Ray S. Review - Synthesis of cast metal matrix particulate composites. J Mater Sci 1998;28:5397-5413.

[7] http://mmc-assess.tuwien.ac.at/ (Database for the Assessment of Metal Matrix Composites for Innovations).

[8] Hashim J, Looney L, Hashmi MSJ. Metal matrix composites: production by the stir casting method. J Mater Process Technol 1999;92-93:1-7.

[9] Segurado J, Gonzáles C, Llorca J. A numerical investigation of the effect of particle clustering on the mechanical properties of composites. Acta Mater 2003;51:2355-2369.

[10] Deng X, Chawla N. Modeling the effect of particle clustering on the mechanical behavior of SiC particle reinforced Al matrix composites. J Mater Sci 2006;41:5731-5734.

[11] Lloyd DJ. Aspects of fracture in particulate reinforced metal matrix composites. Acta Metall Mater1991;39(1):59-71.

[12] Nair SV, Tien JK, Bates RC. SiC reinforced aluminium metal matrix composites, Int Met Rev 1985:30(6):275-290.

[13] Youssef YM, Dashwood RJ, Lee PD. Effect of clustering on particle pushing and solidification behavior in TiB_2 reinforced aluminium PMMCs. Compos Part A 2005;36:747-763.

[14] Reeves AJ, Dunlop H, Clyne TW. The effect of interfacial reaction layer thickness on fracture of titanium-SiC particulate composites. Metall Trans A 1992;23:977-988.

[15] Oh SY, Cornie JA, Russel KC. Wetting of ceramic particulates with liquid aluminum alloys: Part II. Study of wettability. Metall Trans A 1989;20A:533-541.

[16] Naher S, Brabazon D, Looney L. Computational and experimental analysis of particulate distribution during Al-SiC MMC fabrication. Compos Part A 2007;38:719-729.

[17] Ravi KR, Sreekumar VM, Pillai PM, Mahato C, Amaranathan KR, Arul kumar R, Pai BC. Optimization of mixing parameters through a water model for metal matrix composites synthesis. Mater Des 2007;28:871-881.

[18] Rana F, Dhindaw BK, Stefanescu DM. Optimisation of SiC particles dispersion in aluminium metal matrix composites. AFS Trans 1989;255-264.

[19] Delannay F, Froyen L, Deruyttere A. Review – The wetting of solids by molten metals and its relation to the preparation of metal-matrix composites. J Mater Sci 1987;22:1-16.

[20] Rohatgi PK, Asthana R, Das S. Solidification, structure and properties of metal-ceramic particle composites. Int Met Rev 1986;31(3):115-139.

[21] Hashim J, Looney L, Hashmi MSJ. Particle distribution in cast metal matrix composites- Part I. J Mater Process Technol 2002;123:251-257.

[22] Rumpf H. The strength of granules and agglomerates. New York: Agglomeration, Interscience, 1962. p.379-413.

[23] Tomas J. Adhesion of ultrafine particles – A micromechanical approach. Chem Eng Sci 2007;62:1997-2010.

[24] Falk ML, Langer JS. Dynamics of viscoplastic deformation in amorphous solids. Phys Rev E 1998;57:7192-7205.

[25] Schuh CA, Lund AC. Atomistic basis for the plastic yield criterion of metallic glass. Nat Mater 2003;2:449-452.

[26] Mayr SG. Activation Energy of Shear Transformation Zones - A Key for Understanding Rheology of Glasses and Liquids. Phys Rev Lett 2006;97:195501.

[27] Fan Z, Bevis MJ, Ji S. PCT Patent 1999;WO 01/21343 A1.

[28] Ji S, Fan Z, Bevis MJ. Semi-solid processing of engineering alloys by a twin-screw rheomoulding process. Mater Sci Eng A 2001;299:210-217.

[29] Fang X, Shao G, Liu YQ, Fan Z. Effects of intensive forced melt convection on the mechanical properties of Fe containing Al-Si based alloys. Mater Sci Eng A 2007;445-446:65-72.

[20] Lee JC, Byun JY, Park SB, Lee HI. Prediction of Si contents to suppress the formation of Al_4C_3 in the SiC_p/Al composite. Acta Mater 1988;46:1771-1780.

[31] Handbook of Mixing Technology. Schopfheim: EKATO Ruhr- und Mischtechnik GmbH, 1991.

[32] Nagata S, Mixing Principles and Applications. New York: Wiley, 1975. p.250-258.

[33] Lacey PMC. Developments in the theory of particulate mixing. J Appl Chem 1954;4:257-268.

[34] Rogers A. Statistical Analysis of Spatial Dispersions: The Quadrat Method. London: Pion, 1974.

[35] Lacey PMC. Trans Inst Chem Eng 1943;21:53.

[36] Harnby N, Edwards MF, Nienow AW. Mixing in the process industries, 2nd edition. Oxford: Butterworth-Heinemann, 1997. p.25-41.

[37] Curtis JT, McIntosh RP. The interrelations of certain analytic and synthetic phytosociological characters. Ecology 1950;31:434-455.

[38] Karnezis PA, Durrant G, Cantor B. Characterization of reinforcement distribution in cast Al-alloy/SiC_p composites. Mater Charact 1998;40:97-109.

[39] Akhalaghi F, Lajevardi A, Maghanaki HM. Effects of casting temperature on the microstructure and wear resistance of compocast A356/SiC_p composites: a comparison between SS and SL routes. J Mater Process Technol 2004;155-156:1874-1880.

[40] Nagarajan S, Dutta B, Surappa MK. The effect of SiC particles on the size and morphology of eutectic silicon in cast A356/SiC_p composites. Compos Sci Technol 1999;59:897-902.

[41] Gupta M, Lai MO, Soo CY. Effects of type of processing on the microstructure features and mechanical properties of Al-Cu/SiC metal matrix composites. Mater Sci Eng A 1996;210:114-122.

[42] Bindumadhavan PN, Chia TK, Chandrasekaran M, Wah HK, Lam LN, Prabhakar O. Effect of particle-porosity clusters on tribological behavior of cast aluminium alloy A356-SiC_p metal matrix composites. Mater Sci Eng A 2001;315:217-226.

[43] Kendall K. Agglomerate strength. Powder Metall 1988;31(1):28-31.

[44] Lee YJ, Feke DL, Manas-Zloczower I. Dispersion of titanium dioxide agglomerates in viscous media. Chem Eng Sci 1993;48(19):3363-3372.

[45] Rauwendaal C. Polymer Extrusion, 3rd edition, New York: Hanser Publisher, 1985.

[46] Mondolfo LF. Aluminum alloys: Structure and Properties. London: Butterworths, 1976.

[47] Villars P, Calvert LD (Eds.). Pearson's Handbook of Crystallographic Data for Intermetallic phases, 2nd edition. Ohio: ASM International, Materials Park, 1991.

Captions

Figure 1. Schematic illustration of the mixing equipment used for (a) the distributive mixing process and (b) the Rheo-process.

Figure 2. Application of the Quadrat method. Only particles inside and in contact with the left and bottom side of each quadrat are counted.

Figure 3. Typical microstructures of A356 – 5vol.% SiC_p (4μm particle size) (a) compo-cast and (b) HPDC and inset in higher magnification.

Figure 4. Schematic illustration of the fluid flow characteristics in the twin-screw machine. (a) '*Figure 8*' flow pattern along the axial direction, (b) flow pattern on the cross-section of the screws and (c) flow pattern on the axial section [28].

Figure 5. Typical microstructures of A356 – 5vol.% SiC_p (4μm particle size) (a) MC-cast, (b) MC-HPDC.

Figure 6. A356/SiC_p 4μm MC-HPDC composite and micrographs showing the microstructures in different regions of the tensile sample.

Figure 7. Microstructure of a MC-HPDC A356-5vol.% SiC_p composite showing the presence of SiC particles in the aluminium matrix grains (dark in contrast particles inside the white Al-matrix).

Figure 8. A356/SiC_p 4μm MC-HPDC composite SEM micrographs showing (a) the presence of α-AlFeMnSi intermetallic compounds in the microstructure and (b) the very fine, sub-micrometer eutectic Si particles.

Figure 9. The effect of shearing time on the Lacey Index M.

Figure 10. Experimental results from the Quadrat analysis for HPDC and MC-HPDC samples and the theoretical distribution curves.

Figure 11. The effect of shearing time on the skewness β of the particle distribution in die-cast composites.

Figure 12. Comparison of mechanical properties of A356/SiC_p 4μm composites obtained from different processes.

Table1. The effect of processing conditions on the Vickers Hardness of the composites.

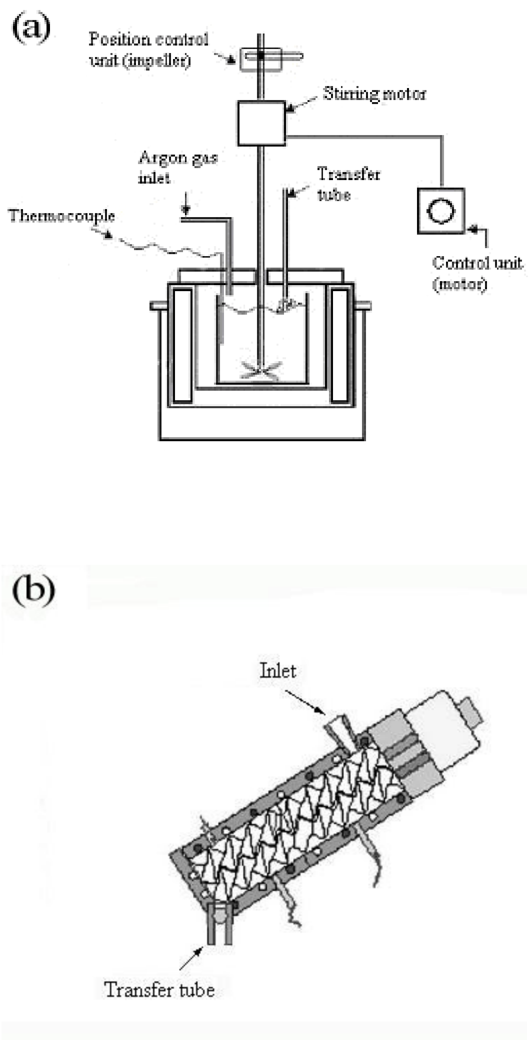

Figure 1. Tzamtzis *et al.*

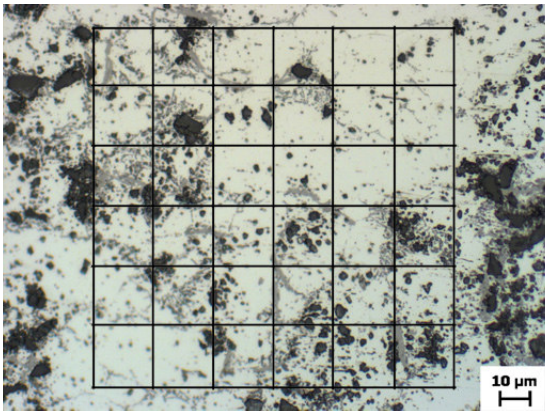

Figure 2. Tzamtzis *et al.*

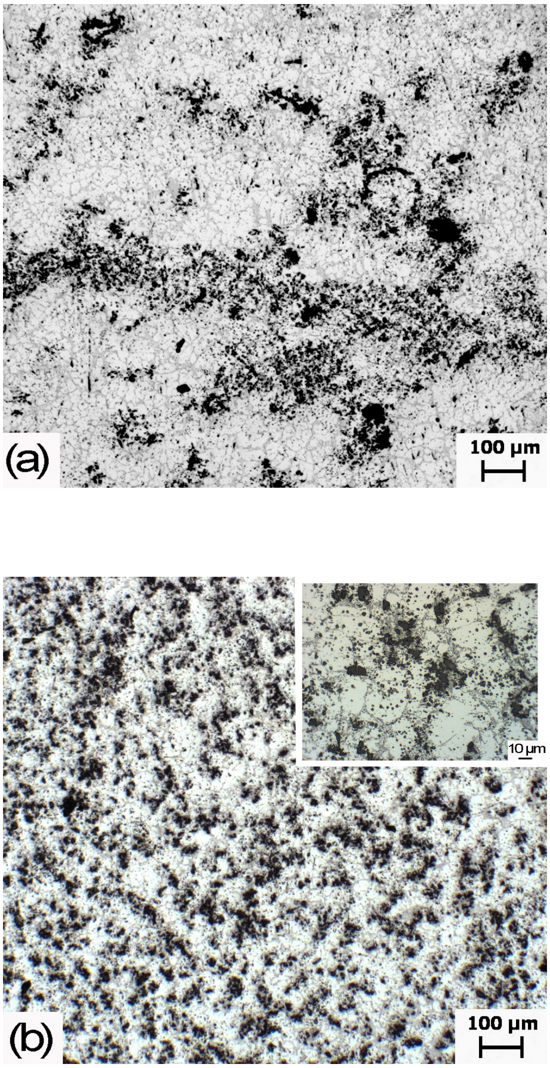

Figure 3. Tzamtzis *et al.*

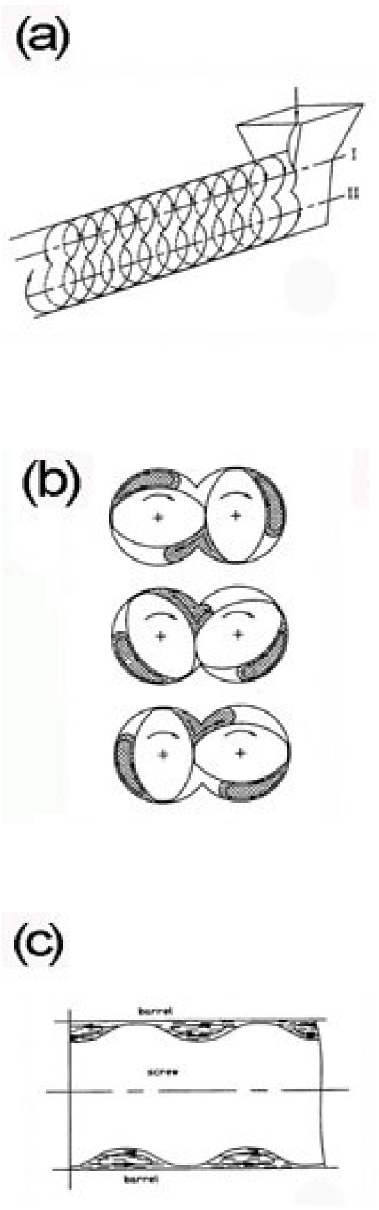

Figure 4. Tzamtzis *et al.*

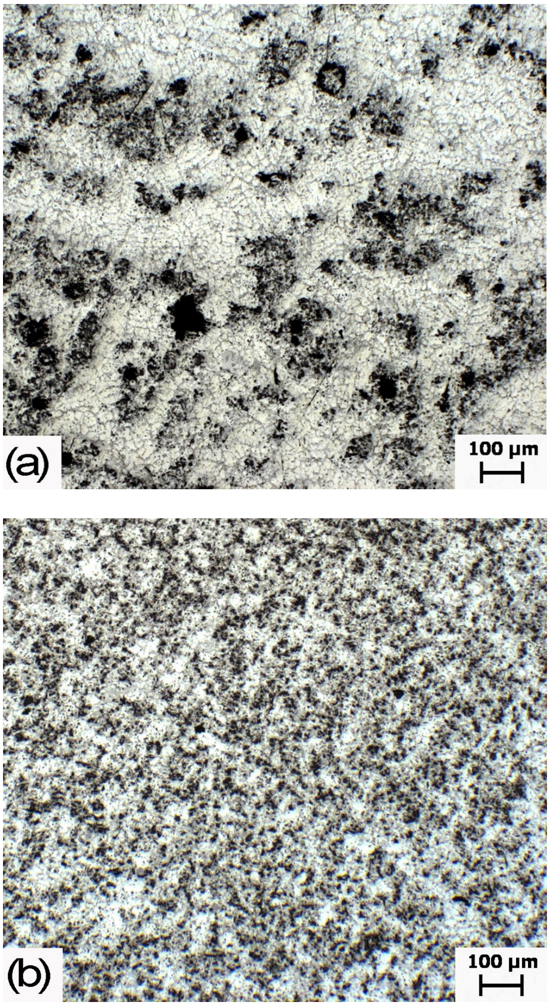

Figure 5. Tzamtzis *et al.*

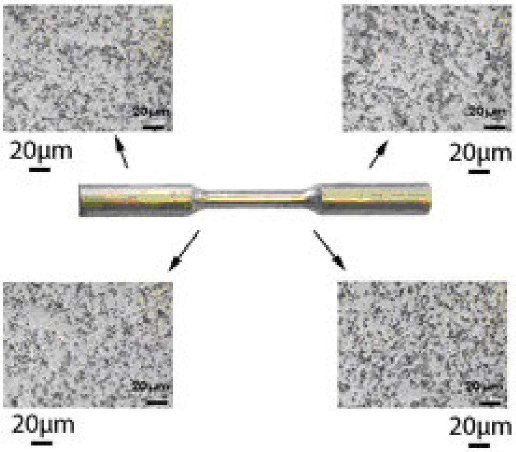

Figure 6. Tzamtzis *et al.*

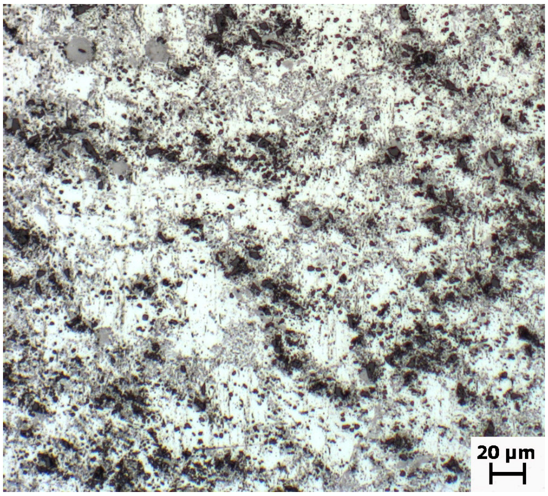

Figure 7. Tzamtzis *et al.*

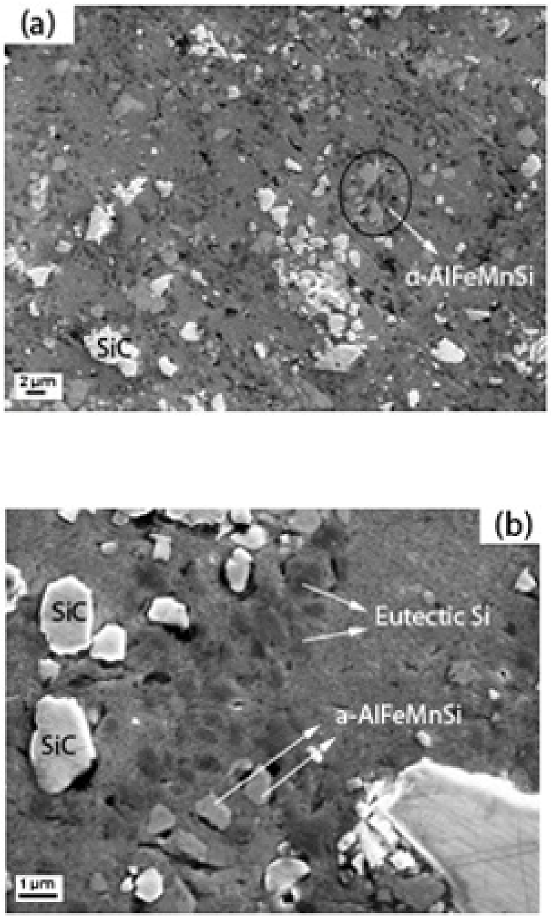

Figure 8. Tzamtzis *et al.*

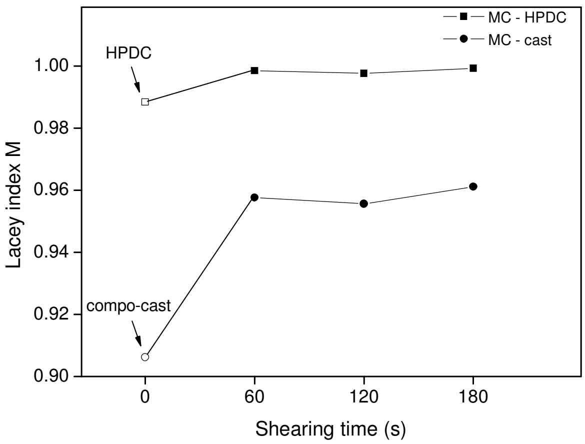

Figure 9. Tzamtzis *et al.*

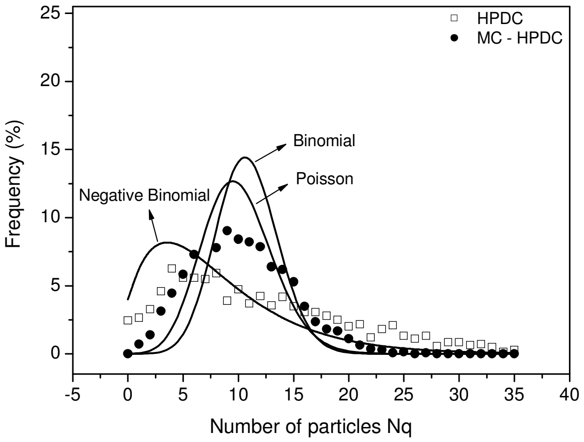

Figure 10. Tzamtzis *et al.*

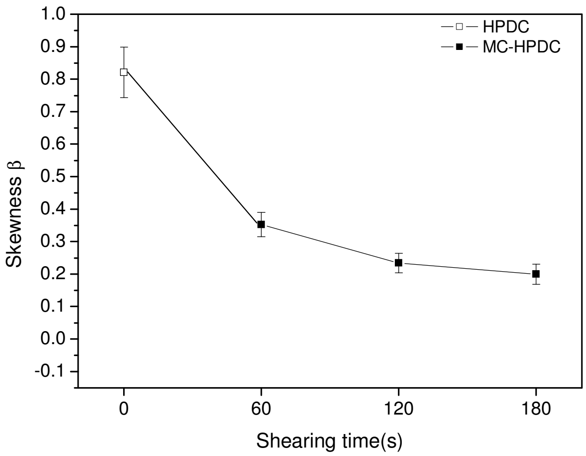

Figure 11. Tzamtzis *et al.*

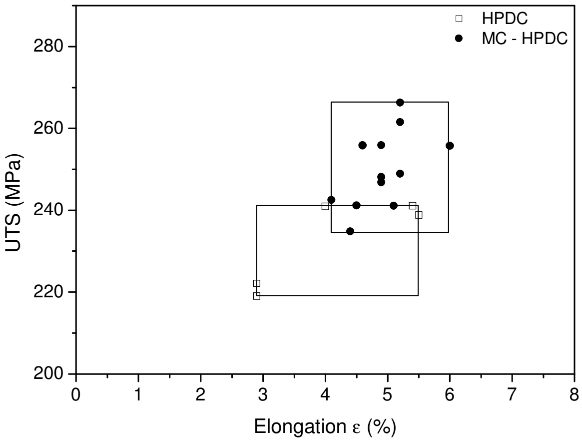

Figure 12. Tzamtzis *et al.*

Casting method	**Processing conditions**			
	Distributive mixing	**Dispersive mixing (Rheo-process)**		
	0s	60s	120s	180s
Steel mould	58.8	61.2	64.7	69.5
Die-casting	73.6	77.5	75.7	79.1

Table 1. Tzamtzis *et al.*